Sol – Cecatto
Period: Sept. 23 – Sept. 30, 2024

Summary

09/23 – No M/X flare; Fast (=< 500 km/s) wind stream; 4 CME can have component toward the Earth;
09/24 – No M/X flare; Fast (=< 500 km/s) wind stream; 4 CME can have component toward the Earth;
09/25 – M1.3 flare; Fast (=< 600 km/s) wind stream; No CME can have component toward the Earth;
09/26 – M1.4 flare; Fast (=< 500 km/s) wind stream; 2 CME can have component toward the Earth;
09/27 – M1.0 flare; No fast wind stream; 2 CME can have component toward the Earth;
09/28 – No M/X flare; No fast wind stream; 2 CME can have component toward the Earth;
09/29 – M1.0, M1.7, M1.7 flares; Fast (=< 500 km/s) wind stream; 5 CME can have component toward the Earth *;
09/30 – No M/X flare; Fast (=< 500 km/s) wind stream; 3 CME can have component toward the Earth **,*,*;
For.: Fast wind stream for next 1-2 days; for while (55% M, 10% X) probability of M / X flares next 1-2 days; also, occasionally some other CME can present a component toward the Earth.

Resumo

23/09 – Sem "Flare" M/X; Vento rápido (=< 500 km/s); 4 CMEs podem ter componente p Terra;
24/09 – Sem "Flare" M/X; Vento rápido (=< 500 km/s); 4 CME com componente p/ Terra;
25/09 – "Flare" M1.3; Vento rápido (=< 600 km/s); Sem CME dirigido para a Terra;
26/09 – "Flare" M1.4; Vento rápido (=< 500 km/s); 2 CME podem ter componente p Terra;
27/09 – "Flare" M1.0; Sem vento rápido; 2 CME podem componente p Terra;
28/09 – Sem "Flare" M/X; Sem vento rápido; 2 CME com componente p Terra;
29/09 – "Flare" M1.0, M1.7, M1.7; Vento rápido (=< 500 km/s); 5 CME podem ter componente p/ a Terra *;
30/09 – Sem "Flare" M/X; Vento rápido (=< 500 km/s); 3 CME podem ter componente para a Terra **,*,*
Prev.: Vento rápido para os próximo(s) 1-2 dia(s); probabilidade de “flares” M/X (55% M, 10% X) nos próximos 1-2 dias; eventualmente alguma(s) outra(s) CME pode(m) apresentar componente dirigida para a Terra.
.

Solar - WSA-ENLIL

EMC (https://ccmc.gsfc.nasa.gov/donki/):

WSA-ENLIL(CME 2024-09-22 21:36:00 UT)
The simulation results indicate that the flank of CME will reach the DSCOVR mission between 2024-09-25 11:00:00 UT and 2024-09-26 01:00:00 UT.

WSA-ENLIL(CME 2024-09-23 20:48:00 UT)
The simulation results indicate that the flank of CME will reach the DSCOVR mission between 2024-09-27 17:00:00 UT and 2024-09-28 07:00:00 UT.

Solar - Coronal holes Spatial Possibilistic Clustering Algorithm (SPoCAS):

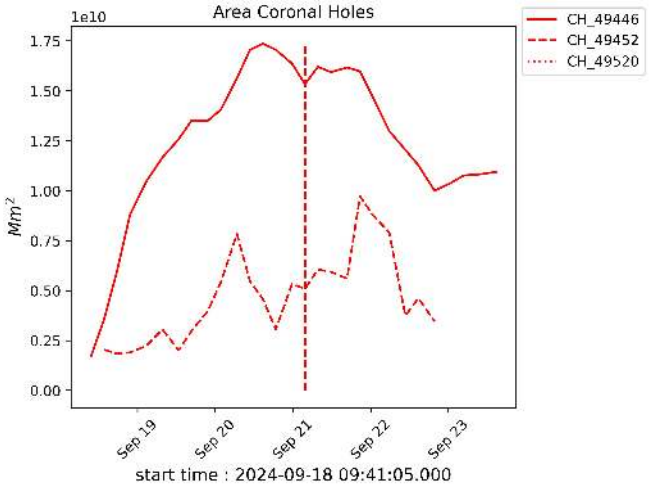

(a) The solid black line depicts the products of the sum of areas for each detection interval performed by SPOCA between September 16 and 23, 2024.

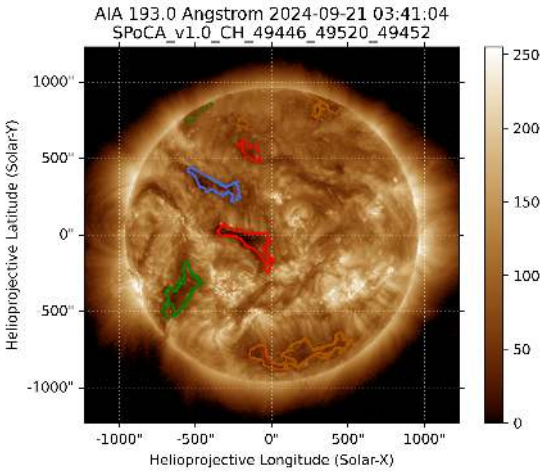

(b) Above the 193 Å image of the Sun are highlighted coronal holes observed by SPOCA around 03:41 UT on September 21, 2024 (red dot line).

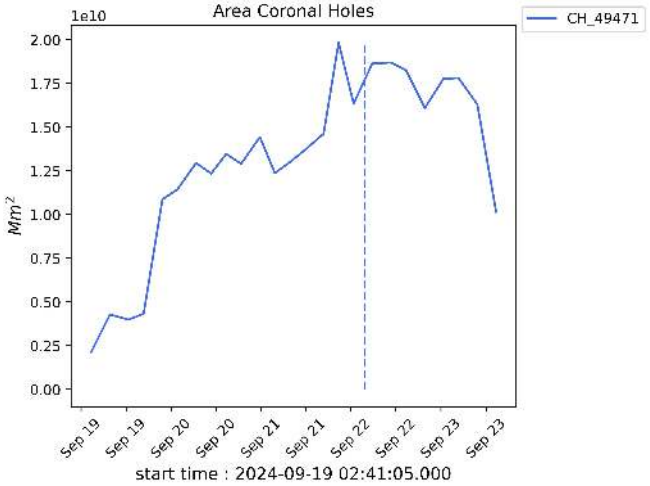

(a) The solid black line depicts the products of the sum of areas for each detection interval performed by SPOCA between September 16 and 23, 2024.

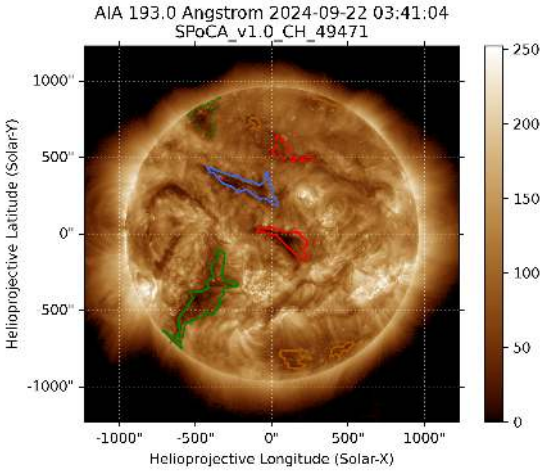

(b) Above the 193 Å image of the Sun are highlighted coronal holes observed by SPOCA around 03:41 UT on September 22, 2024 (blue dot line).

Solar - Coronal holes Spatial Possibilistic Clustering Algorithm (SPoCAS):

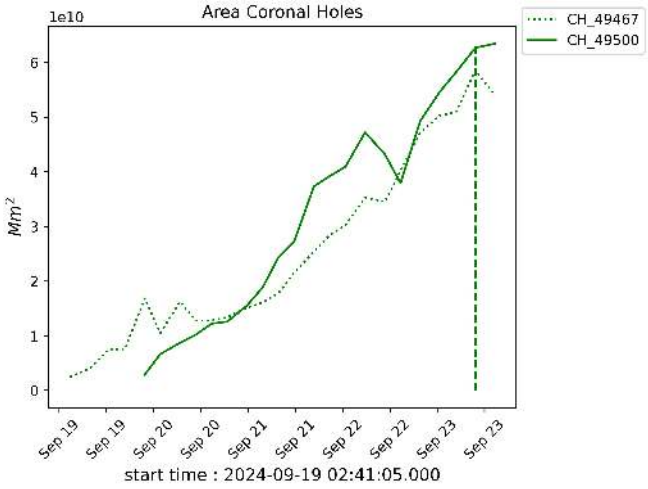

(a) The solid black line depicts the products of the sum of areas for each detection interval performed by SPOCA between September 16 and 23, 2024.

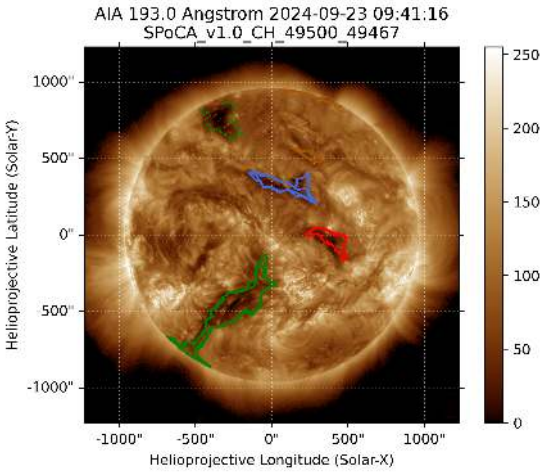

(b) Above the 193 Å image of the Sun are highlighted coronal holes observed by SPOCA around 09:41 UT on September 23, 2024 (green dot line).

EARTH'S RADIATION BELT

Responsible: Ligia Da Silva

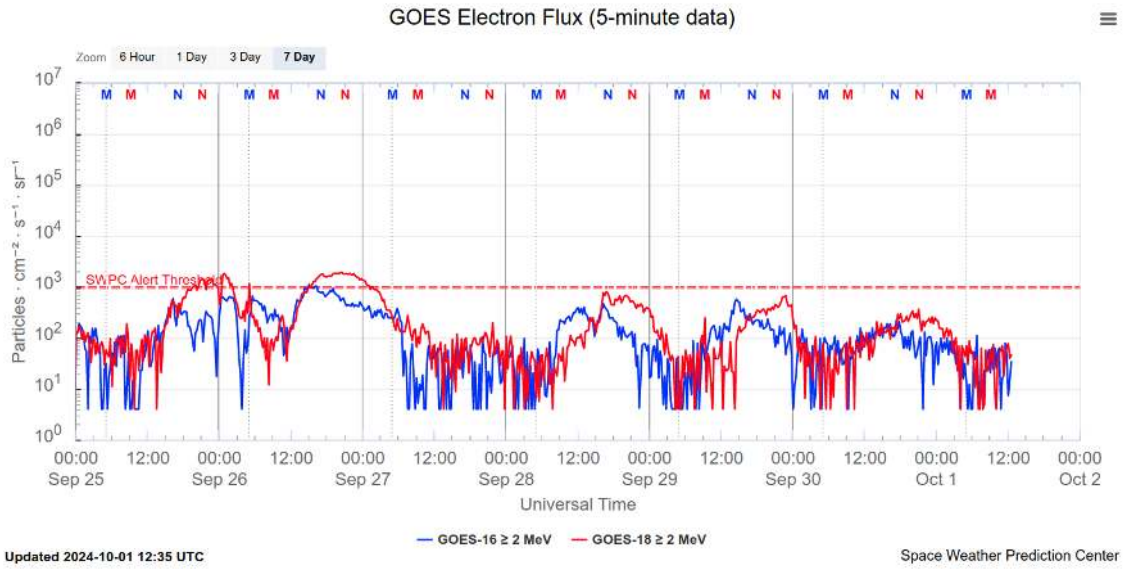

Figure 1: High-energy electron flux (> 2MeV) obtained from GOES-16 and GOES-18 satellite. Source: https://www.swpc.noaa.gov/products/goes-electron-flux

Summary

The high-energy electron flux (>2 MeV) in the outer boundary of the outer radiation belt obtained from geostationary satellite data GOES-16 and GOES-18 (Figure 1) shows an increase, reaching values above 10^3 particles/(cm^2 s sr) from the end of September 25th to the beginning of September 27th. A dropout was observed between September 27th and 28th, followed by a slight increase in flux, which persisted slightly below 10^3 particles/(cm^2 s sr) until the end of the analyzed period. The variabilities of electron fluxes are associated with the arrival of solar wind structures in the magnetosphere.

Geomagnetic Field

Responsible: Karen Sarmiento/ Lívia Alves

Summary

The geomagnetic field reached a minor storm level G1 on September 25, returning to calm conditions by September 27, followed by an increase in activity until unstable conditions were observed on September 30.

On the night side, the GOES magnetometers recorded a decrease in the magnetic field early on September 25, reaching 41 nT at 5 UT, indicating an intensification of currents in the magnetotail. This was followed by rapid fluctuations in the magnetic field, which persisted until 8 UT the next day. On September 29, rapid variations were also observed on the night side, lasting until 11 UT. Auroral activity exhibited instabilities, with the AE index varying between 1000 nT and 1500 nT in two intervals: 13–14 UT on September 23 and 15–17 UT on September 25. Additionally, fluctuations between 500 nT and 1000 nT occurred during several other periods, with a clear signature of substorms. The maximum Kp index was 5- on September 25 (3–6 UT), reaching the minor storm level G1. The Dst index recorded a minimum value of -47 nT on September 25 (21 UT), indicating an intensification of the ring current due to the Bz component of the interplanetary magnetic field, which remained negative (up to -6 nT) from the beginning of September 25 until the end of September 27. The Embrace-Magnet network magnetometers recorded rapid variations in the H component of the magnetic field from noon on September 23 until the end of September 25, as well as between 12–18 UT on September 28 and 29, but without a geomagnetic storm signature. The H component reached a maximum of approximately 118 nT at 14 UT on September 29 at the Porto Velho (PVE) station, located in the influence region of the Equatorial Electrojet (EEJ).

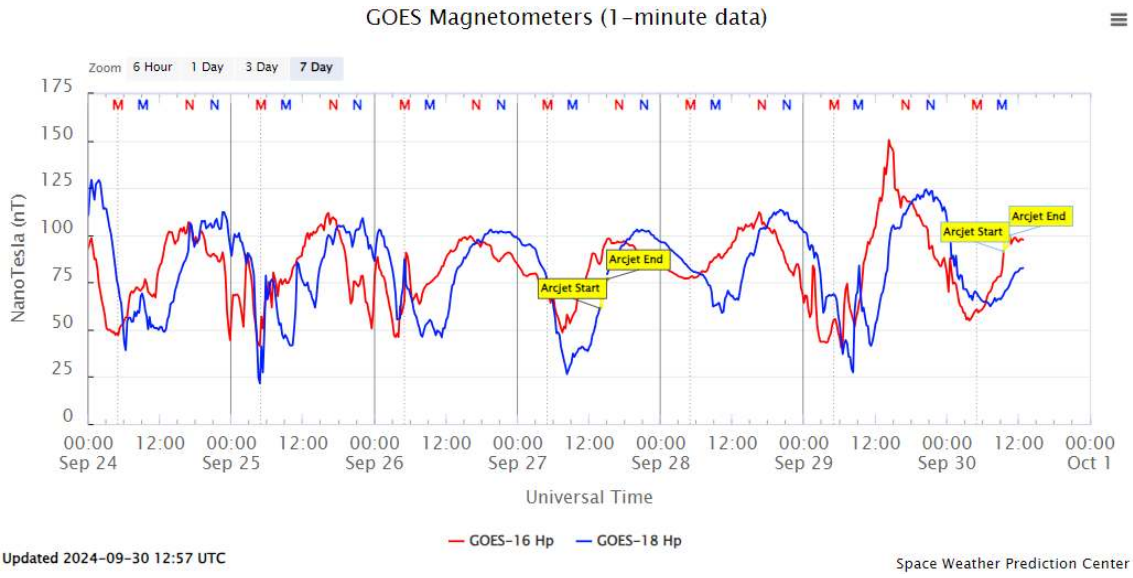

Figure 1- Magnetic field horizontal component at the GOES satellite orbit through.

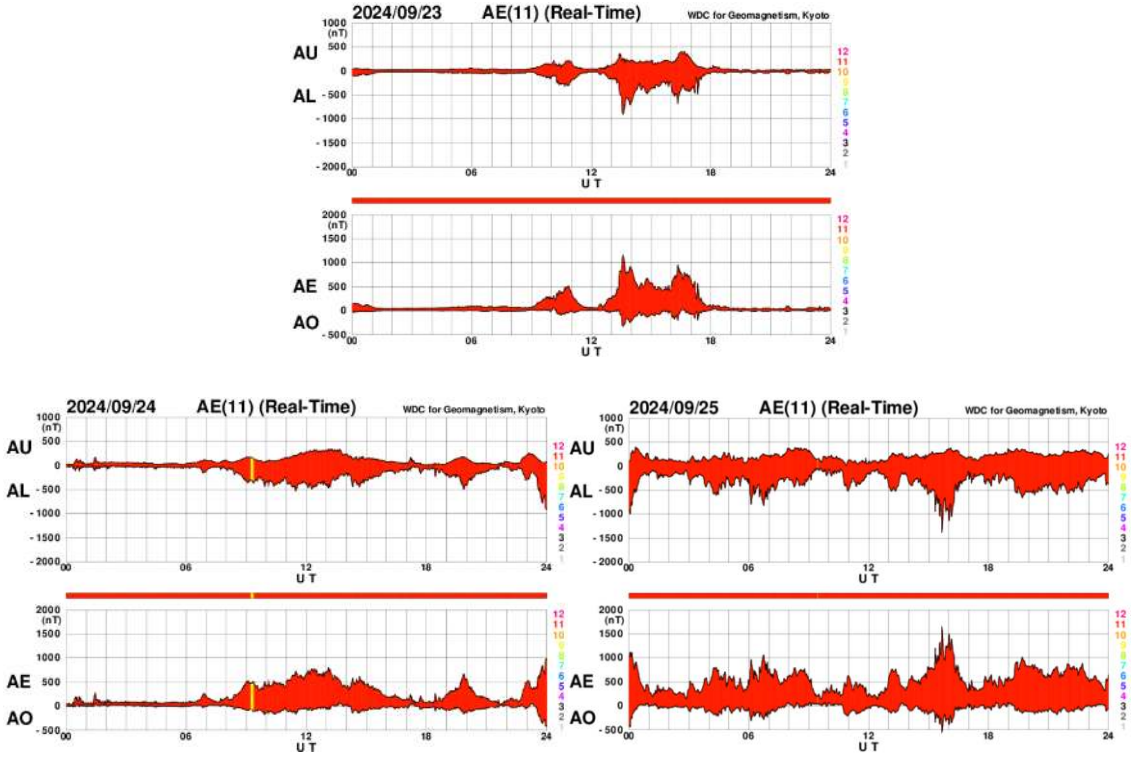

Figure 2- AE index for the days of the week with greater auroral activity.

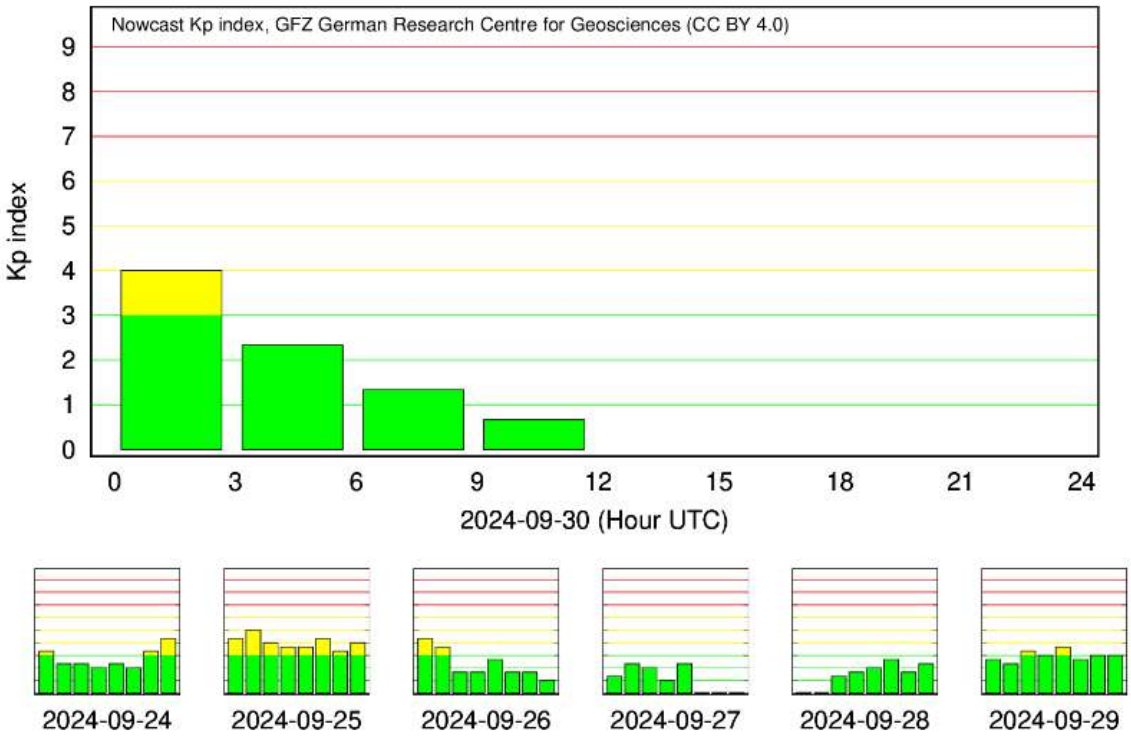

Figure 3- Kp index in logarithmic scale.

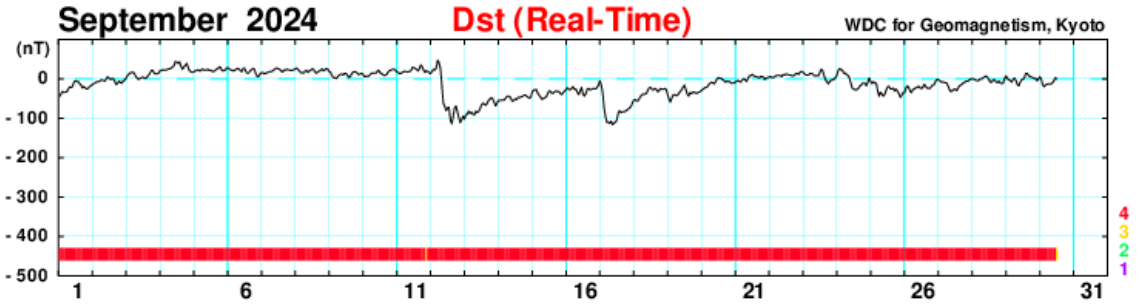

Figure 4- Dst Index

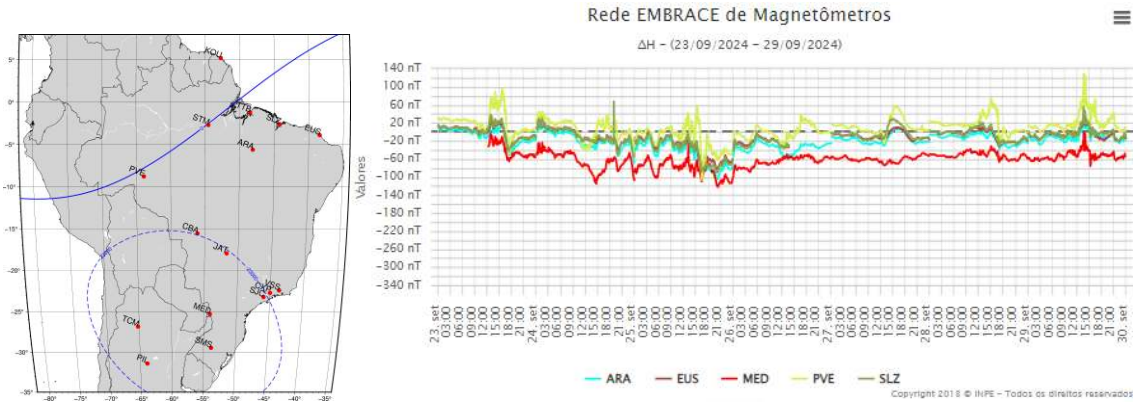

Figure 5- Daily variation of the geomagnetic field from H(nT) measured at Embrace MagNet.

Ionosphere - ROTI
Summary for Week 2333 (September 22 to 28, 2024)

Carolina de Sousa do Carmo

In the week 2333 (September 22 to 28, 2024), ionospheric irregularities (plasma bubbles) were observed during all nights except on September 25, 2024. The Figure below shows the ROTI time series for four stations in the Brazilian sector (Natal (RNNA), Bacabal (MABB), Cuiabá (CUIB), and São José dos Campos (SJSP)).

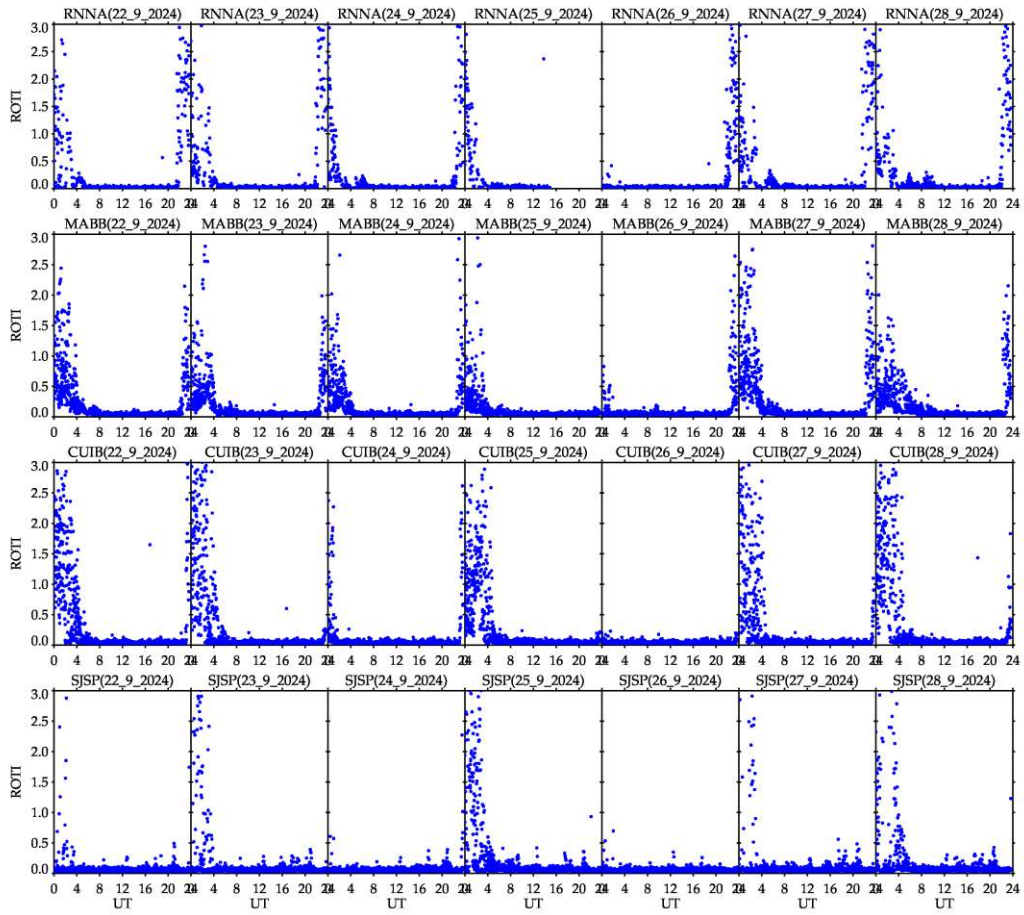

Figure – ROTI time series for four stations in the Brazilian sector (Natal (RNNA), Bacabal (MABB), Cuiabá (CUIB), and São José dos Campos (SJSP)), from September 22 to 28, 2024.